European Congress on Computational Methods in Applied Sciences and Engineering
ECCOMAS 2000
Barcelona, 11-14 September 2000

THERMO-MECHANICAL MODEL OF A STRAND IN THE MOULD OF A CONTINUOUS CASTING PLANT

Frédéric Pascon[*], Anne-Marie Habraken[*], Michel Bourdouxhe[†], and Françoise Labory[†]

[*] Mechanics of Structures and Materials Department (MSM)
Université de Liège
Bat. B52/3, Chemin des Chevreuils, 1, B-4000 Liège (Belgium)
e-mail: F.Pascon@ULg.ac.be , Anne.Habraken@ULg.ac.be
web page: http://www.msm.ulg.ac.be/www/

[†] PROFIL ARBED Recherches
Rue de Luxembourg, 66, L-4009 Esch-sur-Alzette (G.D. Luxembourg)
e-mail: Michel.Bourdouxhe@arbed-rech-isdn1.restena.lu,
Francoise.Labory@arbed-rech-isdn1.restena.lu

Key words: Continuous casting, Solidification, Mould taper, Finite element.

Abstract. *Surface and internal quality of continuous casts depends very much on the behaviour of the strand in the mould. Among the parameters likely to influence this behaviour, the mould taper takes a prominent part. In order to understand better the influence of this parameter, we build up a thermal-mechanical finite elements model. A slice of the strand is modelled and its evolution is observed. The main results are temperature field and solidification evolution, stress, strain and strain rate fields and losses of contact and returns to contact analysis. The model includes an elastic-viscous-plastic law to describe the behaviour of steel from liquid to solid state, a thermal-mechanical element that takes into account thermal expansion and mechanical behaviour of the strand, a unilateral contact element, a mobile rigid boundary element to model the mould and its taper and an adapted loading element to model the ferrostatic pressure according to the liquid or solid state. This paper presents the first results obtained with an relatively simple section (a 125 mm square billet). Now the model is used with more complex sections (beam blanks) and its validation is going on.*

1 INTRODUCTION

Continuous casting is the link between steelmaking and hot rolling processes. This modern technique is more and more important on the steel producers market because of its advantages compared to the older technique of ingots casting: energy and manpower savings, a better yield and improvement of steel quality.

The process can be schematically described as follows (see Figure 1): liquid steel is brought in a ladle to a tundish where it is poured. Several nozzles in the bottom of the tundish allows the liquid steel to flow into as many bottomless moulds, avoiding oxidation. The copper moulds are kept at a relatively constant temperature thanks to a water cooling system. Liquid steel in contact with the mould hardens and a solidified shell starts to grow. This is called the primary cooling. Under the mould, some extracting rolls pull the strand out of the mould and make it moving forward in the machine. Water spray devices are placed between the rolls to continue the cooling of the strand and the solidification process. This is called the secondary cooling. As fast as the strand is moving down the system, the thickness of the solidified shell grows until all of the section is solidified. Then the strand can be cut and sent to storage.

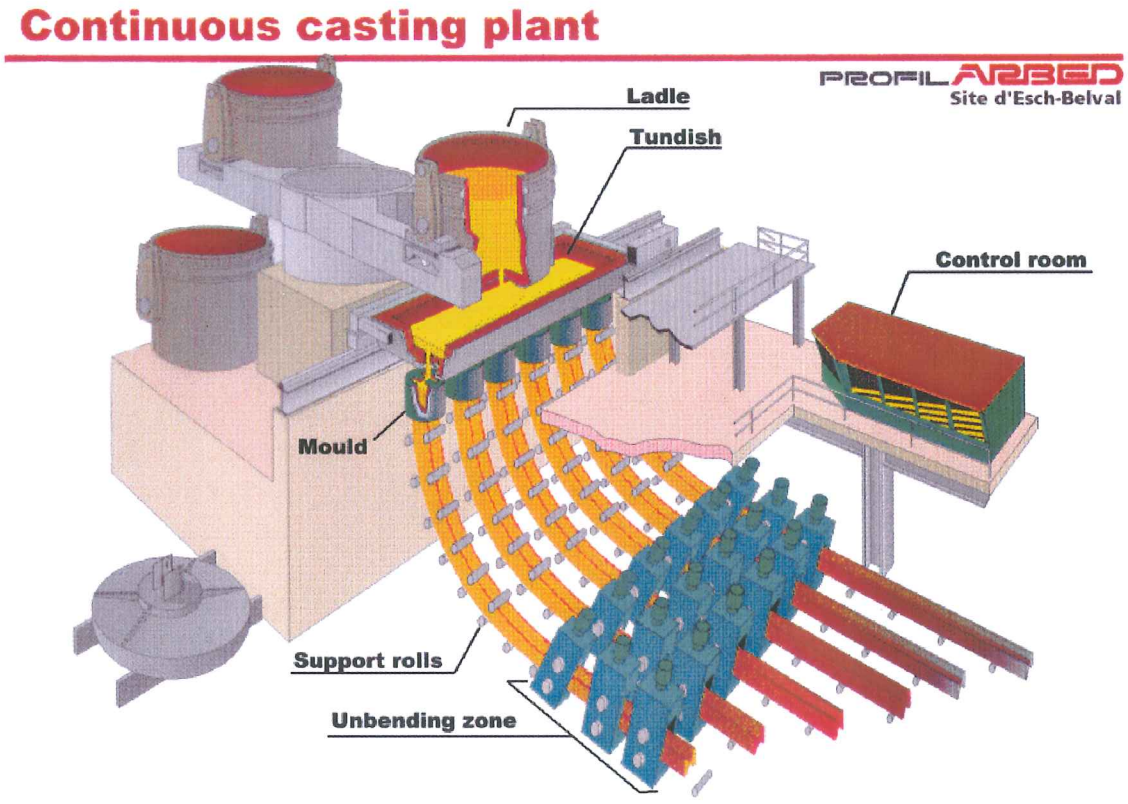

Figure 1: General overview of the continuous casting process

Even if productivity leads producers to speed up the casting process, an appropriate casting speed remains an important factor of quality. If the speed is too high, the strand stays less time in the mould and the solidified shell is too thin, so that surface and subsurface cracks can appear or the strand can even break out. On the other hand, if the speed is too low, the solidified shell grows too much and that may lead to problems in the bending zone.

The mould taper takes also a prominent part in this process [1-3]. In the case of totally convex sections (such as billets and blooms), the taper is positive on the whole outline. If the taper is too low, the contact between the strand and the mould can be lost and a gap appears, leading to a decreasing thermal exchange and defects. At the opposite, if the taper is too high, friction between the strand and the mould induces stresses and strains in the fragile solidifying shell. The consequences can be surface defects also in this case. For more complex cross sections (i.e. beam blanks), the taper can be negative on a part of the outline. In the same way, a wrong taper design can be responsible of quality problems.

Many other parameters are also important for the quality of the product [4-7]. Among these parameters, one can mention steel chemistry and cleanliness, mould level, mould powder, mould oscillation, liquid steel temperature and the overall secondary cooling conditions. The purpose this study is to make a finite element model that describes the thermal-mechanical behaviour of the strand in the mould. This analysis is based on an finite element approach, using the Lagrangian LAGAMINE code that has been developed since early eighties in the MSM Department of University of Liège. More precisely we wanted to determinate for a given situation the temperature field, the stress and strain fields and the contact/friction between the strand and the mould.

2 MODEL DESCRIPTION

2.1 Approach of the problem

A complete three-dimensional seemed to be impossible (both because of numerical stability and convergence reasons, but also computing time), so a "two and a half" dimensional analysis was carried out. One can summarize this approach as follows: we model in a 2D mesh a set of material points representing a slice of the strand, perpendicularly to the strand axis. Initially the strand is at the meniscus level and its temperature is assumed to be uniform and equal to the casting temperature (1560 °C). Since this slide is moving down through the mould, we study heat transfer, stress and strain development and solidification growth.

From a mechanical point of view, the slice is in generalized plane strain state. That means that the thickness t of the slice is governed by the following equation where 3 degrees of freedom α_0, α_1 and α_2 appear:

$$t(x,y) = \alpha_0 + \alpha_1 x + \alpha_2 y \tag{1}$$

So there is a virtual node with coordinates $(\alpha_0,\alpha_1,\alpha_2)$ that is not a material point but it is only representative of the thickness of the studied slice. The coefficient α_0 represents the thickness at the origin of the axes, while α_1 and α_2 are the slopes of the thickness value

respectively along the axes *x* and *y*.

In our model, we considered that the coefficients α_1 and α_2 are constant during the simulation and equal to zero. That means that the thickness is only determined by the value of α_0, so that we can say that the thickness is uniform in the slice but variable in time. This assumption is a consequence of the double symmetry of the studied slice (see hereafter).

By using a variable thickness in time, we can compute an equation for this "third geometric degree of freedom" (the same for each node of the mesh). The generalized plane strain state is thus more complete than classical plane states (plane strain or plane stress states), even if it is not as complete as the three dimensional state. That is the reason why we call it a "two and a half" dimensional state.

2.2 Geometry of the problem

In a first time, we worked with a simple geometry. We modeled the casting of a 125 mm wide squared billet. In order to avoid stress concentration, we rounded the corners of the section, using a 5 mm curvature radius.

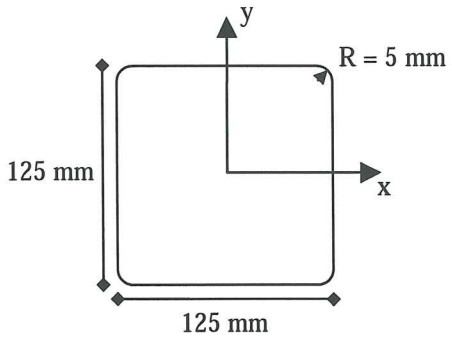

Figure 2: Cross section of the strand

The active height of the mould is 600 mm and the taper is 1.05 % per meter, so that the section is approximately 124.2 mm at the exit of the mould.

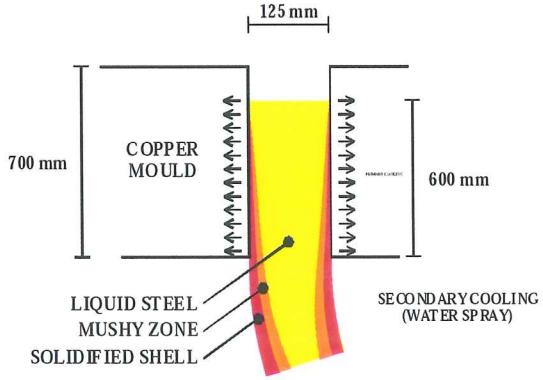

Figure 3: Mould geometry

The initial geometry of the strand is the same than the geometry of the mould (because of the liquid steel) and then it depends on the shrinkage.

Because of the double symmetry, we only studied one quarter of the slice, applying the right boundary conditions along these symmetry axes.

The casting speed is relatively high speed and it is equal to 3.6 meter per minute or 60 mm per second.

2.3 Thermal properties of the material

Liquid steel is pour in the mould at 1560 ℃ (casting temperature). The copper mould is cooled by an internal water flow near the surface. We assumed that the temperature of the mould is constant, uniform and equal to 160 ℃.

The heat flux in the material (the strand) is predicted by a classical Fourier-type law:

$$\rho \cdot c \cdot \dot{T} = \mathrm{div}(\lambda \cdot \nabla T) + q \tag{2}$$

where T is the temperature field, function of coordinates (x,y), ρ is the volumic mass, c the specific enthalpy and λ the thermal conductivity of the material.

The parameter q is a heat source term that is equal to zero in our model, except in the mushy zone where it is equal to the latent heat. In this case, on can express q by the equation:

$$q = \rho \cdot L_s \cdot \frac{\partial f_s}{\partial T} \cdot \dot{T} \tag{3}$$

where L_s is the latent heat of solidification and f_s is the solidified fraction.

In the case of a pure material, the solidification temperature is a single point that makes an infinite derivative. In the case of a non-pure material (such as any steel), the solidification does not occur at a single determined temperature, but only on a phase change interval from the upper temperature (liquidus temperature) to the lower temperature of the domain (solidus). In our model, these temperatures are 1520 ℃ for liquidus and 1470 ℃ for solidus.

Even if the phase change interval is relatively large according to temperature variation during time steps, we used the so-called enthalpy method [8]. We define an enthalpy function H(T), which takes into account all the thermal energy involved in the material to heat it from the absolute zero (0 K) to the considered temperature T (in K):

$$H(T) = \int_0^T \left(\rho \cdot c - \rho \cdot L_s \cdot \frac{\partial f_s}{\partial T} \right) \cdot d\theta \tag{4}$$

The main advantage of this formulation is that the size of time step does not influence the result because the conservation of heat is always verified.

The Fourier law can be written as follows:

$$\dot{H}(T) = \mathrm{div}(\lambda \cdot \nabla T) \tag{5}$$

One can notice that all the parameters (ρ, c, λ, q) are temperature dependant in the model.

2.4 Heat exchange between the strand and the mould

The thermal exchange between the strand and the mould depends very much on the contact conditions. Due to the thermal shrinkage, contact may be lost in some places, more particularly in the corners, as Figure 4 shows. When contact is lost, the thermal exchange decreases and the core of the strand tends to reheat the solidified shell so that the strand bulges and returns to contact with the mould.

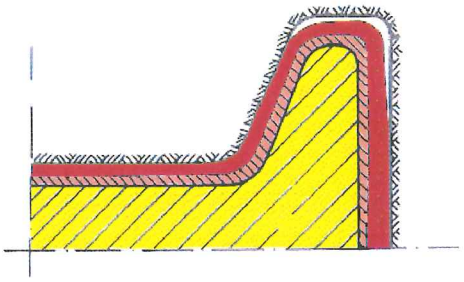

Figure 4: Gap appearance in the corners

Where the contact between the strand and the mould is established, the heat transfer q is based on the following expression:

$$q = R \cdot \left(T_{strand} - T_{mould}\right) \tag{5}$$

where R is the contact thermal resistance.

Where the contact is lost, a gap appears and the heat transfer is given by:

$$q = h \cdot \left(T_{strand} - T_{mould}\right) + \varepsilon_r \cdot \sigma_B \cdot \left(T_{strand}^4 - T_{mould}^4\right) \tag{5}$$

where h is the heat transfer coefficient of convection mode, ε_r the relative emissivity of the strand and σ_B the Boltzmann radiation constant.

2.5 Mechanical properties of the material

The main mechanical effect of solidification is shrinkage the value of which is directly proportional to the thermal decreasing. The proportionality coefficient is the thermal expansion coefficient α and it is also thermally affected. During a time step, the thermal part of strain rate is given by:

$$\dot{\varepsilon}^{therm} = \alpha(T) \cdot \dot{T} \cdot \begin{pmatrix} 1 & 0 & 0 \\ 0 & 1 & 0 \\ 0 & 0 & 1 \end{pmatrix} \tag{6}$$

The mechanical behaviour of the material is described by a elastic-viscous-plastic law for both liquid, mushy and solid states.

The elastic domain is characterized by an elastic Young's modulus E and a lateral

contraction coefficient ν (Poisson's coefficient) that are temperature dependant.

The viscous-plastic domain is described thanks to a Norton-Hoff type law the expression of which is:

$$\hat{\dot{\varepsilon}}_{ij}^{vp} = \frac{\left(J_2\right)^{\frac{1-p_3}{p_3}} \cdot \left(\bar{\varepsilon}\right)^{-\frac{p_4}{p_3}} \cdot e^{\frac{p_1 \cdot \bar{\varepsilon}}{p_3}}}{2\left(K_0 \cdot p_2\right)^{\frac{1}{p_3}}} \cdot \hat{\sigma}_{ij} \tag{7}$$

This expression allows to model both hardening and softening and an implicit integration scheme has been used. In terms of equivalent values, the formulation becomes:

$$\bar{\sigma} = K_0 \cdot e^{-p_1 \cdot \bar{\varepsilon}} \cdot p_2 \cdot \sqrt{3} \cdot \left(\sqrt{3} \cdot \bar{\dot{\varepsilon}}\right)^{p_3} \cdot \bar{\varepsilon}^{p_4} \tag{8}$$

where K_0, p_1, p_2, p_3, p_4 are temperature dependant parameters. Each parameter has its own influence on the curve shape:

- K_0 and p_2 influence the level of the curve;
- p_1 is mostly influent when $\bar{\varepsilon}$ is higher, in other words influence on softening;
- p_4 works on hardening;
- p_3 traduces the effect of strain rate, i.e. viscosity.

The variation of these parameters as functions of temperature allows to model the variation of mechanical behaviour of the material, including viscosity. Each parameter has been fitted at several temperatures corresponding to tensile tests that had been performed on a Gleeble device at several high temperatures (800 °C to 1475 °C) and strain rates (10^{-4} to $5\ 10^{-2}\ s^{-1}$).

The difference between K_0 and p_2 is that K_0 was previously used as yield stress. Now we do not use it anymore because it is only temperature dependant, not strain rate dependant. Indeed, using that can introduce discontinuities in the stress path because the elastic part is unique from zero to the yield stress, but then the viscous-plastic curve can have different levels depending on the strain rate. That's the reason why we compute the yield limit as the intersection between the elastic straight line and the viscous-plastic curve.

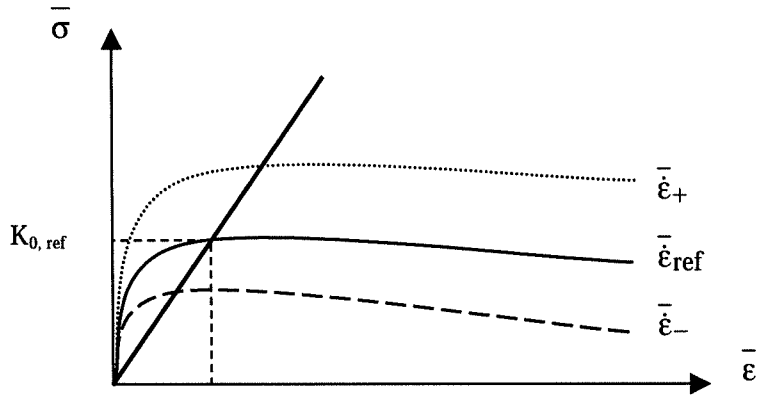

Figure 5: Yield limit depending on the strain rate (at a given temperature)

The ferrostatic pressure p_f is taken into account. In the liquid phase, it given by:

$$p_f = \gamma \cdot D \tag{9}$$

where γ is the volumic weight and D the distance below the meniscus. In the solid phase, the pressure is obviously equal to zero. In the mushy zone, we assume a linear variation. So we can summarize it:

$$p_f = \gamma \cdot D \cdot (1 - f_s) \tag{10}$$

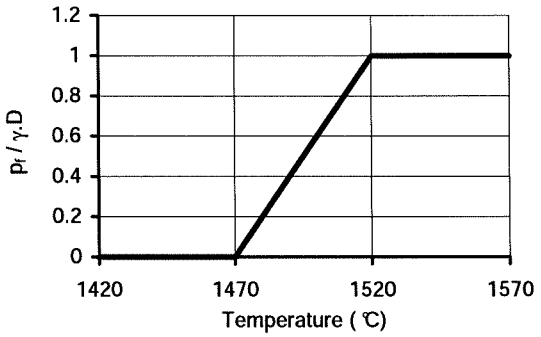

Figure 6: Ferrostatic pressure vs. temperature

When two adjacent elements are in liquid state, the pressures are balanced so that there is no resulting force. But when the pressures are different, a resulting force takes place. In this way, the solidified shell is under ferrostatic pressure because of the liquid steel pool in the core of the strand.

2.6 Mechanical contact

From the mechanical point of view, the contact between the strand and the mould induces both pressure and friction efforts. The chosen contact element [9] is based on a penalty technique and expresses the Signorini's condition at its integration points. The constitutive equation for the contact is a Coulomb-type law [10].

2.7 Discretization

The strand, more precisely the studied quarter of slice, is modeled with quadratic quadrangular elements (8 nodes) and 4 integration points with Gauss scheme for each element. The elements are of course larger in the center of de slice and the smallest near the corner where most of the stresses and strains will grow. The mesh is composed of 560 nodes and 168 volume elements. Each node owns three degrees of freedom (coordinates *x* and *y* and temperature T).

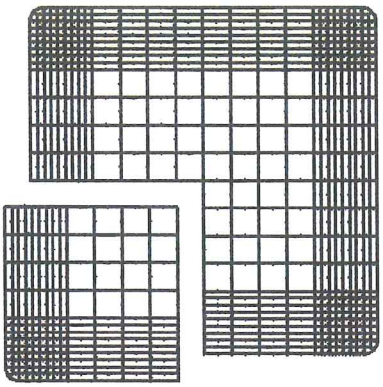

Figure 7: mesh for the studied quarter of slice

The contact (or loss of contact) between the mould and the strand is modeled using 3 nodes contact elements. The particularity of these contact elements is that they use a three dimensional law, even if the analysis is only two dimensional. The reason of this is that we want to take into account the friction in the casting direction, that is to say perpendicularly to the studied slice.

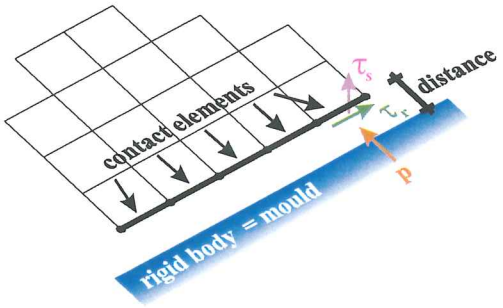

Figure 8: pressure and frictional efforts

The mould is represented by a rigid body so that its thermal distortion is not take into account. The geometry of the mould at each time step is defined by the taper that we impose. It can be a single, multiple or parabolic taper.

2.8 Coupling of the analysis

The resolution of the problem is achieved thanks to a "partly" coupled analysis. The principle depend on two parallel analysis, a purely mechanical one and a purely thermal one. After a fixed interval of time, data are exchanged between the two analyses.

This method was necessary because of very expensive CPU time in the case of a fully coupled analysis. It has been used many times previously for different kinds of problems and what has been concluded is that the results are not too much affected. The more frequent the data exchange are, the closer to the fully coupled analysis the results are, but the CPU time becomes longer and longer. A good compromise should be found. In our case, data are

exchanged every 0.25 s for an overall time simulation of 10 s, that is to say 40 data exchanges.

3 RESULTS

3.1 Temperature at the exit of the mould and growing of the solidified shell

Figure 9 represents some isotherms in the slice at the exit of the mould. Temperature decreases to circa 1200 ℃ in the corner, while it is still greater than 1500 ℃ in most of the central zone (casting temperature is 1560 ℃).

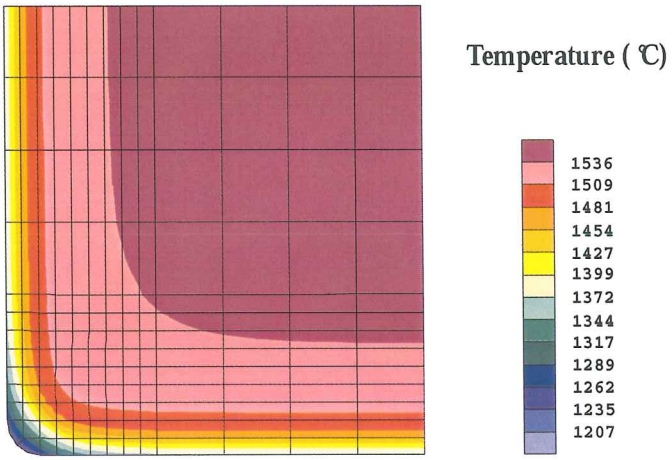

Figure 9: Temperature at the exit of the mould

One of the most interesting result is the thickness of the solidified shell. The thickness of the three different phases (liquid, mushy and solid) are given at the exit of the mould by the Figure 10:

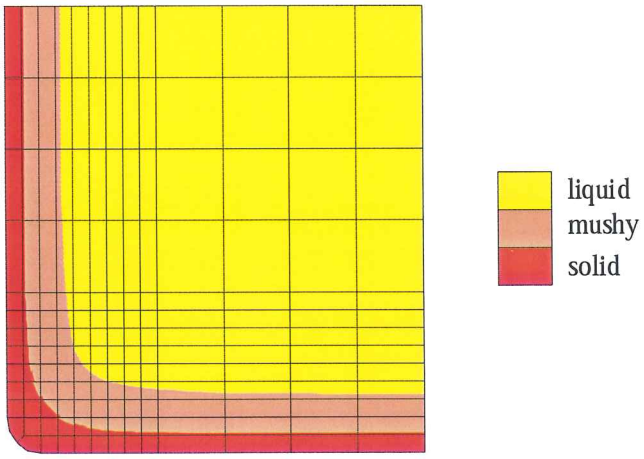

Figure 10: The three different phases at the exit of the mould

These values are given by the isotherms at 1470 ℃ (solidus) and at 1520 ℃ (liquidus).The thickness of the solidified shell is circa 3 mm and the one of the mushy zone is circa 5.5 mm. These values are close to reality (about 5 mm for each zone), but still too low for the solidified shell. This difference may be due to the thermal exchange coefficients that are relatively rough in a first time.

The previous figures are representative of the state of the slice at the exit of the mould but we can also want to know what happens during the simulation. If we measure along a principal axis the evolution of the thickness of these three phases during the simulation, we obtain the Figure 11. These thickness are deduced from the moving of the solidus and liquidus isotherms.

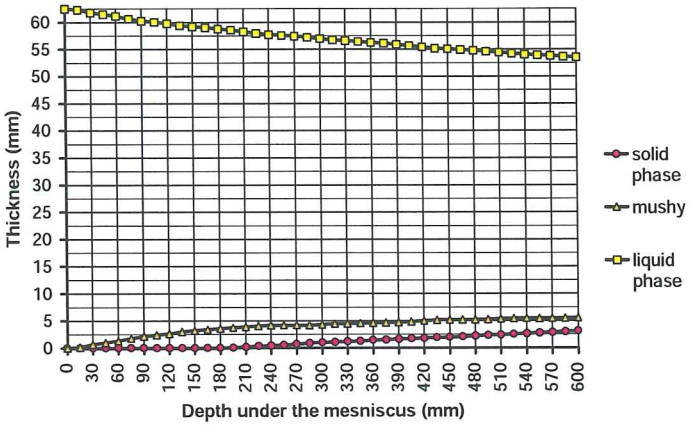

Figure 11: Evolution of the thickness of the three phases until the exit of the mould (600 mm under meniscus)

On this figure we can clearly see that the mushy zone grows immediately, while the solidified shell appear about 200 mm uunder the meniscus.

3.2 Stress, strain and strain rate fields

The following figures represent the stress, strain and strain rate fiels in the slice at the exit of the mould. We do not analyse here these results in terms of absolute values because there is no interest to do that with this exemple. We just verify that the behaviour seems to be correct and that what we attempt to do is achieved.

Figure 12 shows the Von Mises equivalent stress field. Similarly to the temperature field, it is obvious that the maximum equivalent stresses are in the corner, in other words in the solidified zone. The reason is that the material is able to withdraw to larger loads in this region. Conversely, the liquid poll cannot withdraw and the stress in this area tends to zero.

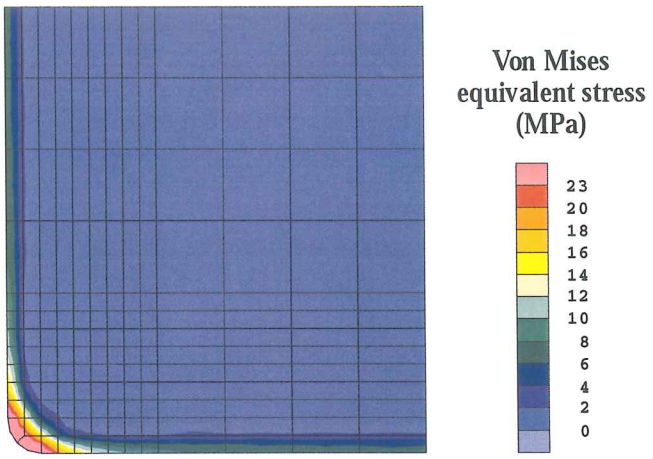

Figure 12: Von Mises equivalent stress field at the exit of the mould

Most of the strain is a thermal effect so the larger values are where the temperature decrease the most (in the solidified shell), as Figure 13 shows. In other respects, a corner effect appears: the equivalent is smaller in the corner than elsewhere on the surface.

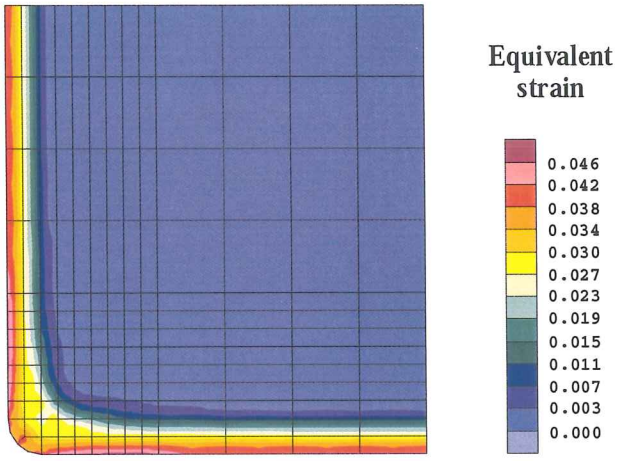

Figure 13: Equivalent strain field at the exit of the mould

Finally, the equivalent strain rate is given by Figure 14. The strain rate represent the variation of strain during the time step. What we can see is that the maximum value is not in the corner or the solidified zone (conversely to the previous figures), but in the mushy zone. As the principal strain is thermal strain, we can give different reasons to this field:

- first, most of the central region is still liquid and the thermal effect is not very large, so that strain rate is very low;
- in the solidified shell, temperature decreasing is more important, but the material "resistance" is greater than anywhere else and the strain remains low;
- last but not least, in the mushy phase, the temperature decreasing is quite important, but the thermal expansion coefficient is 20 times greater than the one of the solidified material

and 28 times greater than the one of the liquid steel; that means that for a same temperature rate, the strain rate will be 20 or 28 times the one in the other phases.

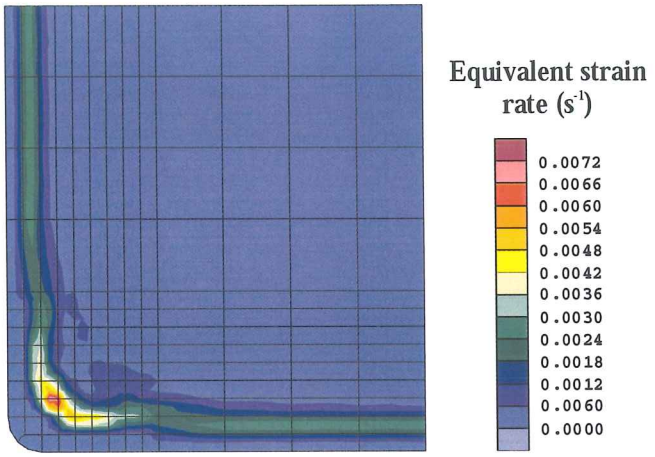

Figure 14: Equivalent strain rate field at the exit of the mould

3.3 Strand-mould contact

An important goal of the study is to manage to model the loss of / return to contact. Figure 15 represent the evolution of the distance between the strand and the mould during the simulation. The value of the distance is positive when there is loss of contact and negative when there is contact. A value can be negative because of the penalty technique in the contact computation.

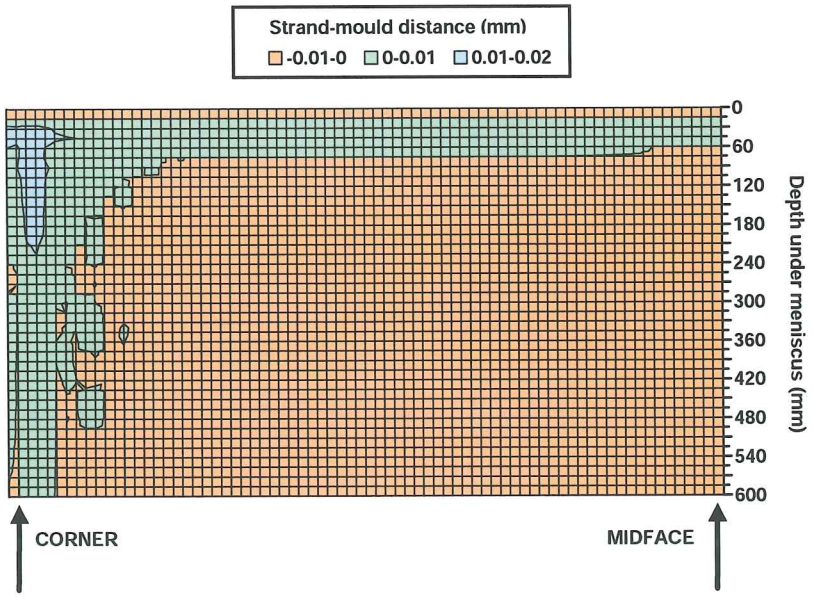

Figure 15: Evolution of the distance between the strand and the mould form the corner to the midface

We can see that in the first time the contact is lost everywhere along the outline of the cross section. Then, the contact returns over a large region (in the central part of the face), and it will not be lost anymore. At the opposite, the contact remains lost in the corner until the exit of the mould (600 mm under the meniscus). Lastly, in a region near to the corner, lost and returns to contact follows each other, that we can see with the orange and green marks.

4 CONCLUSION

The aim of the study was to build up a model of the thermal-mechanical behaviour of a steel strand in the mould of a continuous casting plant. The results we wanted to check were the temperature field and the solidified shell growth, the stress, strain and strain rate fields and finally the ability of the model to manage the loss of contact and returns to contact.

The presented results have been achieved for relatively simple section and the values are not to be put in parallel with experimental tests. But the overall behaviour of the simulated strand accords with what we can expect it should be.

The next step in the study is now to model another shape of strand, like a beam blank for instance, and to compare results with reality. This validation work is going on. Then we will be able to modify different parameters, such as mould taper, casting speed, mould and/or casting temperature, etc.

Acknowledgements

The authors are grateful to the European Coal and Steel Community for this steel research program in collaboration with British Steel Teesside Technology Center, Sidenor I+D and Profil ARBED Recherches. This model development has been achieved thanks to a collaboration between Profil ARBED Recherches and the University of Liège.

REFERENCES

[1] S. Chandra, J.K. Brimacombe and I. Samarasekera, "Mould-strand interaction in continuous casting of steel billets – Part 3 Mould heat transfer and taper", *Ironmakinig and Steelmaking*, 1993, vol. 20, No.2, pp. 104-112.

[2] M.R. Ridolfi, B.G. Thomas and U. Della Foglia, "The optimization of mold taper for the Ilva-Dalmine round bloom caster", *La Revue de Métallurgie – CIT*, Avril 1994, pp. 609-620.

[3] M. Bourdouxhe, A.M. Habraken and F. Pascon, "Mathematical modelisation of beam blank casting in order to optimise the mould taper", *3rd European Conference on Continuous Casting*, October 20-23, Madrid 1998

[4] J.E. Kelly, K.P. Michalek, T.G. O'Connor, B.G. Thomas and J.A. Dantzig, "Initial development of thermal and stress fields in continuously cast steel billets", *Metallurgical Transactions A*, vol. 19A, October 1988, pp. 2589-2602.

[5] M. El-Bealy, N. Leskinen and H. Fredriksson, "Simulation of cooling conditions in secondary cooling zones in continuous casting process", *Ironmaking and Steelmaking*,

1995, vol. 22, No.3, pp. 246-255.

[6] R. B. Mahapatra, J.K. Brimacombe, I. Samarasekera, N. Walker, E.A. Paterson and J.D. Young "Mold behavior and its influence on quality on the continuous casting of steel slabs : Part I. Industrial trials, mold temperature measurements, and mathematical modeling", *Metallurgical Transactions B*, vol. 22B, December 1991, pp. 861- 874

[7] R. B. Mahapatra, J.K. Brimacombe and I. Samarasekera, "Mold behavior and its influence on quality on the continuous casting of steel slabs : Part II. Mold heat transfer, mold flux behavior, formation of oscillation marks, longitudinal off-corner depression, and subsurface cracks", *Metallurgical Transactions B*, vol. 22B, December 1991, pp. 875- 888

[8] C.R. Swaminathan and V.R. Voller, "A general enthalpy method for modeling solidification processes", *Metallurgical Transactions B*, vol. 23B, October 1992, pp. 651-664.

[9] Cescotto S., Charlier R., "Frictional contact finite element based on mixed variational principle", *Int. J. for Numerical Methods in Engineering*, vol. 36, 1993, pp. 1681-1701.

[10] Habraken A.-M., Radu J.-P., Charlier R., "Numerical approach of contact with friction between two bodies in large deformations", *Contact Mechanics International Symposium*, Lausanne, October 92.